Interpretation of Laser Weld Penetration and Welding Phenomena

（Invited Paper）

Seiji Katayama*　　Yousuke Kawahito

（*Joining and Welding Research Institute，Osaka University，Osaka 567-0047，Japan*）

Corresponding author：*katayama@jwri.osaka-u.ac.jp*

Abstract　Deeply penetrated welds can be produced with high-power-density lasers. Thus the factors affecting laser weld penetration，laser-induced plume behavior and the interaction between a laser beam and a plume，keyhole behavior，melt flows in the molten pool，and the generation and prevention of bubbles and porosity were investigated. Consequently，the effects of plasma and plume on the weld penetration were interpreted in CO_2 and fiber lasers welding，respectively. The formation of spattering，underfilled beads，and humping was understood. It was confirmed that porosity was easily formed at high powers and low welding speeds due to the generation of many bubbles from the tip of a keyhole.

Key words　laser welding；CO_2 laser；fiber laser；laser welding phenomena；weld penetration

CLCN：TV547.6　　　　**Document Code**：A　　　　**doi**：10.3788/CJL20093612.3160

1　Introduction

Laser welding has gained great popularity as promising joining technology with high quality，high precision，high performance，high speed，good flexibility，and low deformation or distortion，in addition to the recognition of easy and wide applications due to congeniality with a robot，reduced manpower，full automation，systematization，production lines，etc[1]. Applications of laser welding are increasing. The defects or drawbacks of lasers and their welding are the high costs of laser apparatuses，difficult melting of highly reflective or highly thermal-conductive metals，small gap tolerance，and easy formation of welding defects such as porosity in deeply penetrated weld fusion zones.

Therefore，to understand the mechanism of weld penetration and the phenomena in CO_2，YAG，or fiber laser welding，a variety of researches have been performed concerning laser-induced plume behavior，the interaction between a laser beam and its induced plume/plasma，melt flows，keyhole behavior，and bubbles generation in the molten pool leading to the porosity formation in the weld fusion zones[2~26].

2　Experimental Procedures

Welding with high-power CO_2，YAG，or fiber lasers was performed on Type 304 austenitic stainless steel or aluminum alloy plates，and their weld penetration and welding phenomena were compared. The behavior and characteristics of a laser-induced plume and/or plasma，and the interaction between a laser beam and a plume were observed or measured by using high speed video cameras，spectroscopic measurement，and probe laser beams. An example of the observation system for visualization of interaction between the laser beam and the plume during welding is shown in Fig. 1[2,3]. A 1090-nm fiber laser，830-nm diode laser，and 630-nm He-Ne laser are used as probe beams during YAG or fiber laser welding.
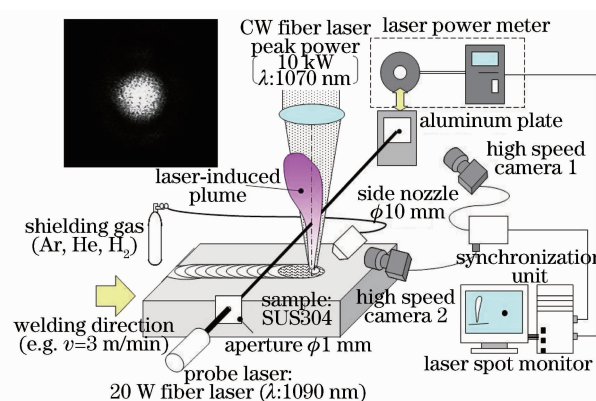

Fig. 1　Schematic of observation and measurement system for visualization of interaction between probe laser beam and laser-induced plume during laser welding

Keyhole behavior，bubble formation，melt flows，and molten pool geometry were also observed through an X-ray transmission real-time imaging apparatus，as shown in Fig. 2[4,5]. For clear visualization of pool geometry，a platinum （Pt）

wire was placed in a hole on the surface of Type 304 stainless steel plate. The observation was performed at the framing rate of 1000 F/s.

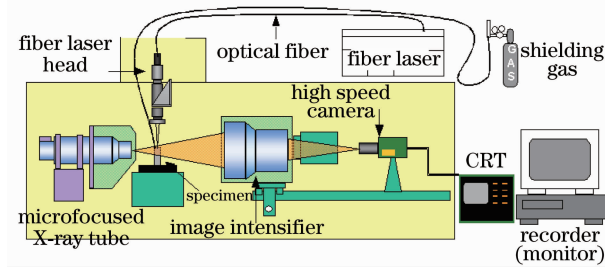
Fig.2 Schematic of a microfocused X-ray transmission in-situ observation system

3 Factors Affecting Laser Weld Bead Penetration

In welding with a continuous wave laser, weld penetration and geometry are affected by the kind of lasers with different wavelengths, laser powers, beam diameters, beam qualities, focused power densities, transverse electromagnetic mode (TEM), defocused distance (laser focusing situation), welding speeds, materials physical properties (laser beam reflectivity, thermal diffusivity, surface tension, and the content of volatile elements), environment such as air, shielding gas kind, gas flow rate and vacuum, laser-induced plasma and plume, and so on[2~26].

Type 304 welds made with a CO_2 laser of 10-kW power in different shielding gases are exhibited in Fig.3[4,5], showing the effect of shielding gas on the penetration. The penetration is deep in He gas, but the depth decreases with the increase in the gas ratio of Ar to He. The penetration is slightly shallower in N_2 gas than He gas.

type 304 (10 mm); bead welding; P_0=10 kW, v=25 mm/s, f_d=±0 mm (f=381 mm), R_g=8.5×10⁻⁴ m³/s

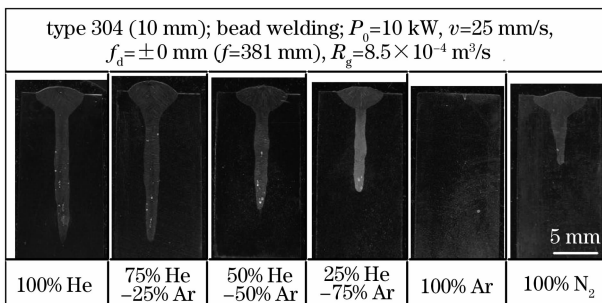| 100% He | 75% He −25% Ar | 50% He −50% Ar | 25% He −75% Ar | 100% Ar | 100% N_2 |

Fig. 3 Cross sections of type 304 weld beads produced with a 10-kW CO_2 laser in different shielding gases

The penetration geometries and depths of weld beads made with a fiber laser with power ranging from 1 to 10 kW in Ar shielding gas are indicated in Fig. 4[6]. The penetration increases with the increase in the laser power. Deeply penetrated welds can be produced in fiber laser welding at high powers even in Ar gas. The comparison of these figures demonstrates that the effect of a shielding gas is more noted at higher powers of 10.6-μm CO_2 lasers, but not so great in welding with YAG or fiber laser with the wavelength of about 1.06 μm.
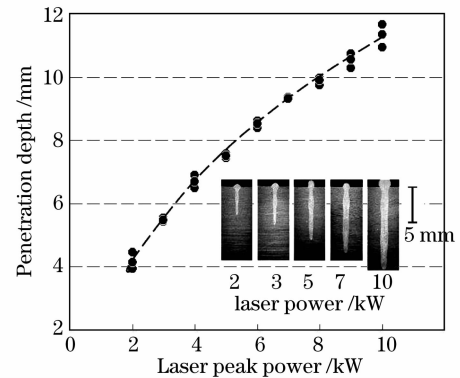

Fig.4 Penetration geometries and depths of type 304 weld beads made with fiber laser power from 1 to 10 kW

The penetration depths in various aluminium alloys are shown as a function of defocused distance in Fig.5[7]. The welds are deep near the focal point because of high power density (5 kW) but becoming shallow at the longer defocused distance. It is understood that deeper penetration can be easily formed in alloys with a larger amount of volatile alloying elements such as Mg and Zn[7~9].
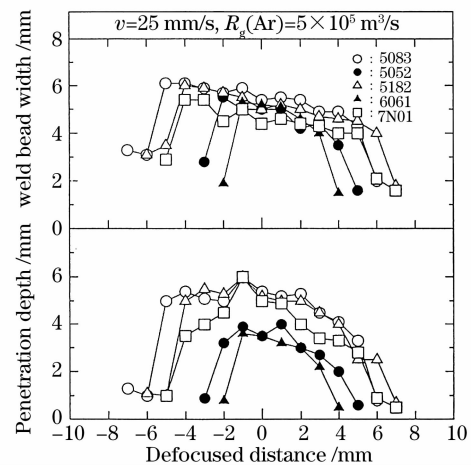

Fig.5 Effect of defocused distance on penetration depths in various aluminium alloys

The penetration depths of weld beads produced with 10-kW fiber lasers with different beam diameters (different power densities) at the focal point are shown as a function of welding speed in Fig. 6[10]. The weld beads are deeper at the slower

welding speeds. It is noted that the higher power densities can produce deeper weld beads at high welding speeds. On the other hand, at lower speeds, the effect of power density on weld penetration is small although the power exerts a great effect on the penetration[10,11].
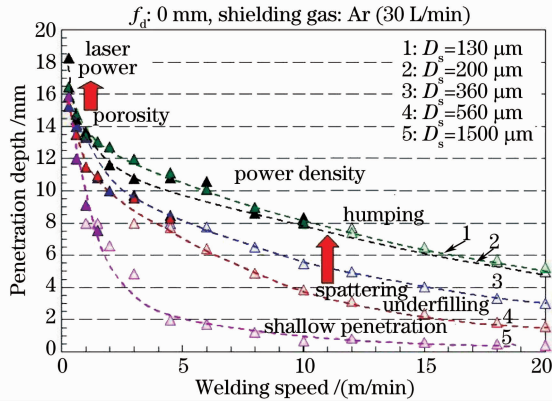

Fig. 6　Effects of beam diameter and welding speed on penetration depths of weld beads produced in type 304 steel with a 10-kW fiber laser

4　Behaviour and Characteristics of Laser-Induced Plume, and Interaction between Laser Beam and Induced Plume during CW Laser Welding

Examples of laser-induced gas plasma and metal plume observed during CO_2 laser welding of A5083 aluminium alloy under the conditions of 5-kW power, 50-mm/s speed, and 30-L/min coaxial flow of He, Ar, and N_2 shielding gas are shown in Fig. 7[12]. In He gas, a plume is only formed by the emission of neutral metal atoms spouting from a keyhole inlet during welding, while in Ar or N_2 gas, gas plasma is always or sometimes formed under the nozzle in addition to the plume from the keyhole, respectively. In welding with CO_2 laser of 10 kW or more in Ar or N_2 side gas, a gas plasma flows up to the laser periodically to block an incident laser beam
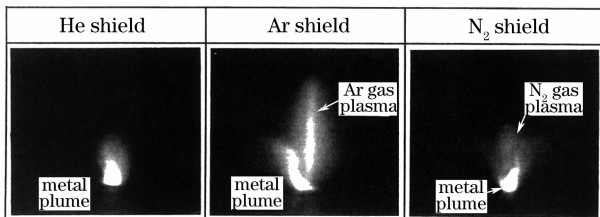

Fig. 7　Plasma and plume observed during CO_2 laser welding of A5083 alloy in He, Ar, and N_2 coaxial shielding gas, showing effect of shielding gas kind on plasma formation

so as to reduce weld penetration, as a welding example at 15-kW power in N_2 side gas demonstrating the relationship between gas plasma formation and keyhole behaviour is shown in Fig. 8[13]. It is interpreted that Ar or N_2 gas plasma is more easily formed because of the lower ionisation potentials in comparison with He gas, and the gas plasma exerts the inverse bremmstrahlung process on the CO_2 laser beam because the effect is proportional to λ^2, where λ is the laser wavelength[14,15].
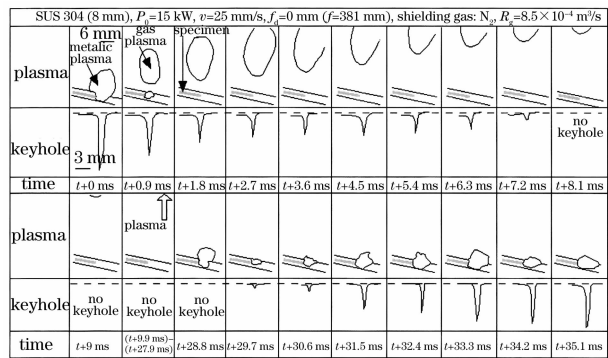

Fig. 8　Simultaneous observation result of phenomena during CO_2 laser welding in N_2 gas, showing the relationship between gas plasma formation and keyhole behavior
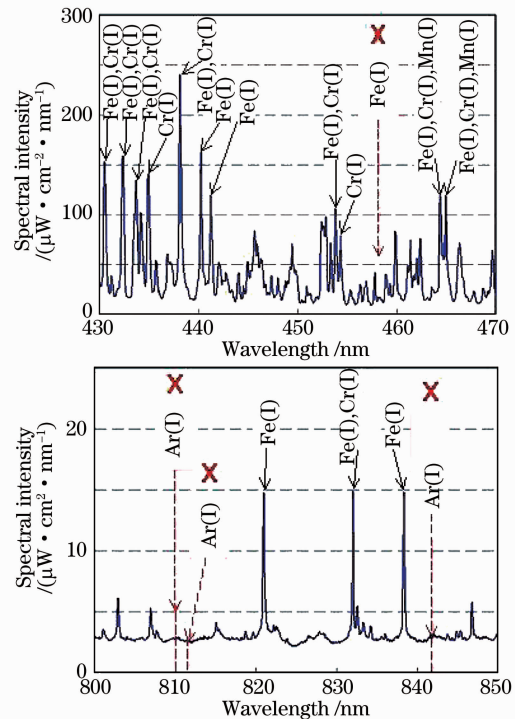

Fig. 9　Spectroscopic measurement and analytical result of plume induced during 10-kW fiber laser welding of type 304 stainless steel

An example of spectroscopic measurement and analysis of a plume during welding of Type 304 stainless steel with a 10-kW fiber laser beam at the

ultra-high power density of about 1 MW/mm² in Ar shielding gas is shown in Fig. 9[6]. Almost all peaks come from the emission of neutral atoms and the emission from Ar gas is not detected. The inverse bremmstrahlung effect seems to be negligibly small in welding with a laser beam of about 1-μm wavelength. According to Saha equation, it is estimated that a plume is in the state of a weakly-ionized plasma (about 6000 K and 2% atomic ions)[6]. Figure 10 shows examples of photos displaying the relationship between plume behavior and probe laser motion[2,6]. It was confirmed that the refraction and attenuation of a probe laser beam existed due to an inclined refraction index profile caused by slanted distribution of vapors density at high temperatures and Rayleigh scattering, respectively[2,11,16,17]. The interaction of such a small-sized plume on a 1.06-μm laser beam was judged to be small.
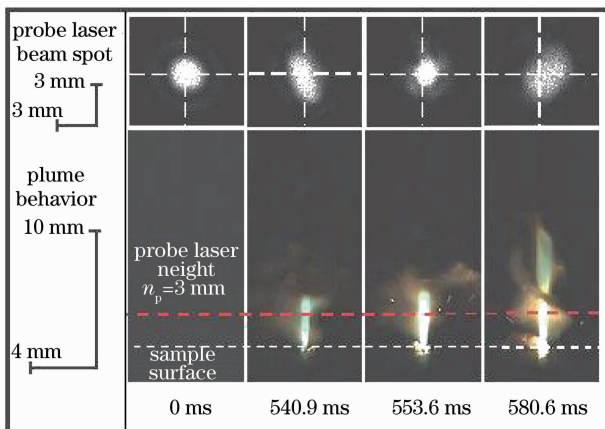

Fig. 10 Simultaneous observation results of probe fiber laser behavior (upper) and laser-induced plume (lower), showing visual interaction between laser beam and laser-induced plume
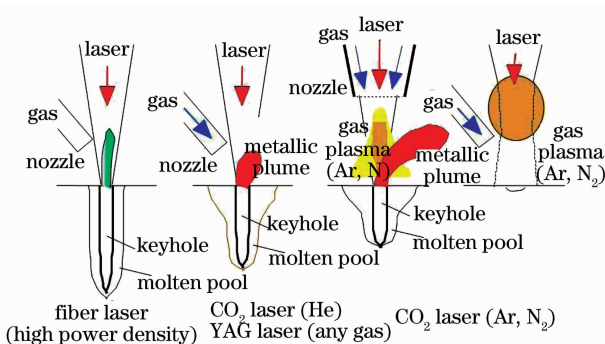

Fig. 11 Schematic plume and plasma behaviour and consequent keyhole in laser weld fusion zone

The plume and plasma behavior and the consequent keyhole geometry in the molten pool are illustrated in Fig. 11[15]. In the case of CO_2 laser of about 10.6-μm wavelength, Ar and N_2 gas forms gas plasma, resulting in the apparent decrease in weld penetration, whilst in the case of YAG, fiber, or disk lasers of about 1-μm wavelength, the shielding gas effect is small, and laser power and its density exert the penetration[10,16].

5 Suppression Procedures of Laser Welding Defects

Welding can be carried out under a variety of conditions by using a high-brightness and high-quality fiber laser. In welding with a moderate high power density of fiber laser, sound weld beads with convex surfaces were produced. On the other hand, underfilled weld beads were formed due to the generation of large spatters at the high welding speed of more than 10 m/min at the lower power density, while the weld beads with humping occurred at high power density (see Fig. 6). To clarify these welding phenomena, high-speed video observation of the surface of a molten pool was performed.

Fiber laser bead-on-plate welding was performed under the welding conditions of 6-kW laser power, ϕ 360-μm spot diameter, and various welding speeds. Examples of the observation results at the welding speed of 6 and 10 m/min are shown in Figs. 12(a) and (b), respectively. At 6 m/min, the molten pool was more than 7 mm in length. A keyhole was located near the front of the molten pool and the melt flowed out from the keyhole inlet to form a convex surface. Large spatters were formed from the melt, but jumped on the large molten pool and disappeared. At the welding speed of 10 m/min, the molten pool became smaller and the spattering became more severe. Almost all melts near the top of the surface formed spatters. Consequently, the underfilled weld bead with large spat-

(a) f_d=0 mm, welding speed: 6 m/min, shielding gas: Ar (30 L/min)

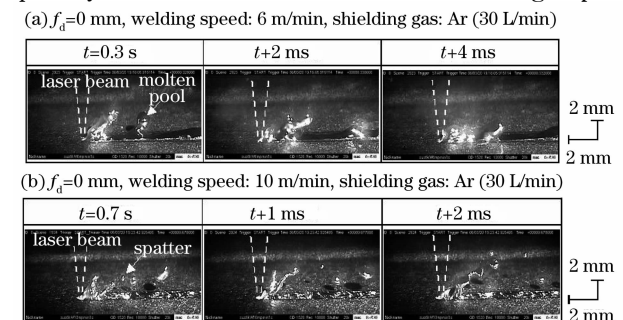(b) f_d=0 mm, welding speed: 10 m/min, shielding gas: Ar (30 L/min)

Fig. 12 High-speed video camera observation results of molten pool surface during fiber laser welding at 6-kW power and 360-μm beam diameter

ters was formed. This mean that spattering can be prevented by a long molten pool.

Figure 13 shows the observation results of the molten pool under the welding conditions of 6-kW laser power，ϕ 115-μm spot diameter，and 6-m/min travelling speed. A Xenon arc lamp was used for illumination to observe the molten pool and laser-induced plume. It was confirmed that the molten pool was very narrow and long，the backward melt flow due to the ejection of laser-induced plume was strong，and the humping part was generated gradually at the rear part of the molten pool. It was considered that the humping was formed due to strong backward melt flow induced by laser plume and higher surface tension with very narrow bead width.
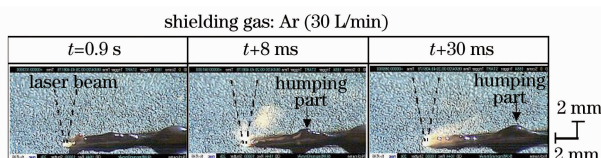

Fig. 13 High-speed video camera observation results of molten pool surface at high power density

Porosity is easily formed in deeply penetrated weld beads at low welding speeds. X-ray transmission observation results confirm that bubbles are generated from a keyhole tip to form porosity at low welding speeds，while bubbles are not formed at high welding speeds，resulting in no porosity，and examples of 6-kW fiber laser welding are shown in Fig. 14[11]. From such observation results，plume behavior，keyhole behavior，melt flows，and bubble generation leading to porosity formation in the molten pool are schematically summarized in Fig. 15[15]. At low welding speeds，a deep keyhole is likely to collapse，then a laser beam is irradiated on the collapsed liquid wall of the keyhole，and consequently downward melt flows are caused by the recoil pressure of evaporation from the collapsed wall. Such phenomena may produce large bubbles leading to pores. As the welding speed is slightly increased，intense evaporation sometimes takes place from the front wall of a keyhole（where the liquid layer is thin）to deform the rear wall of the keyhole（where the liquid is large）so as to produce a bubble. Under a certain condition，bubbles flow upward to disappear from the molten pool surface. If the material has such a high surface tension to produce a stable keyhole，the vapors are strongly ejected
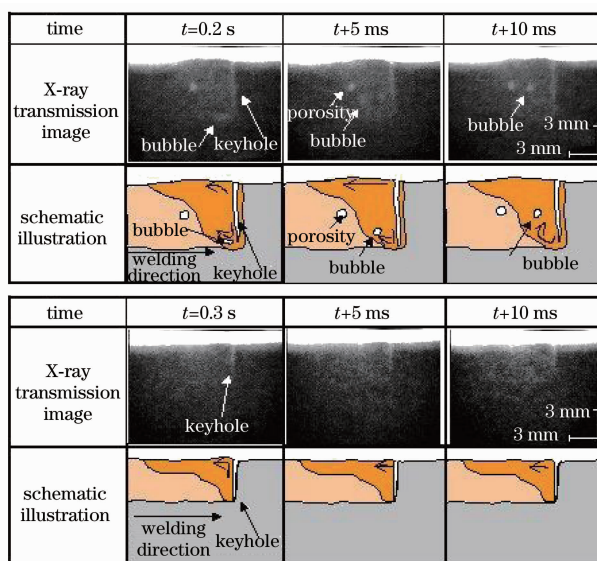

Fig. 14 X-ray transmission observation results and schematic representation of keyhole behaviour，melt flows，bubble formation and molten pool geometry during welding with 6-kW fiber laser at speeds of 1.5 and 6 m/min
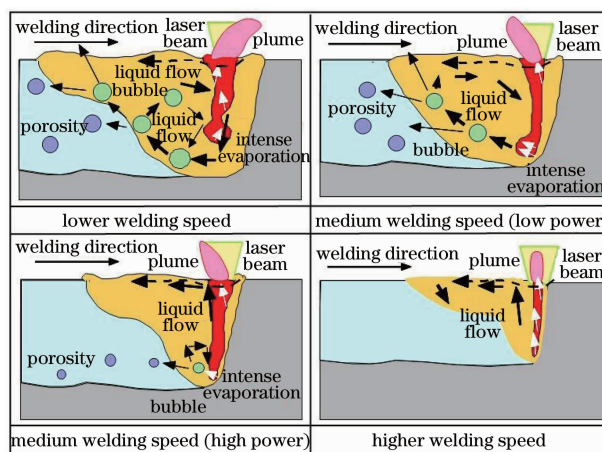
Fig. 15 Schematic representation of plume behavior，keyhole behavior，melt flows，and bubble generation leading to porosity formation in molten pool according to respective conditions

upwards from the keyhole inlet to induce the melt flow near the inlet upward，and smaller bubbles are formed from the keyhole tip. Consequently，pores are present near the bottom part of the weld bead. When the welding speed is high enough，a plume ejects upwards，and a keyhole becomes so stable as to suppress or prevent bubble formation，resulting in reduced or no porosity. At high powers such as 20 to 40 kW in He shielding gas and/or at high power densities（e. g.，10 kW）with 0.2-mm focused beam，bubbles leading to pores are sometimes generated from the middle part of a keyhole.

Examples of X-ray transmission photos during continuous wave（CW）YAG laser welding of Type 304 steel in Ar，He，and N_2 shielding gas are shown in Fig. 16[18]. Bubbles are formed in an inert gas such as Ar and He，but bubbles are hardly seen in N_2. Ar and He gas is generally detected in the pores. Therefore，Ar or He gas is involved in a unstable keyhole at lower welding speeds，but a harmful influence of N_2 is reduced by reacting with Cr vapors in the keyhole or being included due to high solubility in the molten pool. N_2 gas is regarded as a proper shielding gas in YAG，disk or fiber laser welding of austenitic stainless steels.

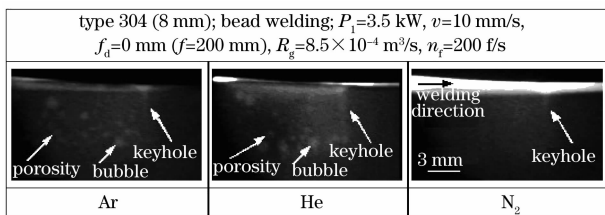type 304 (8 mm); bead welding; P_1=3.5 kW, v=10 mm/s, f_d=0 mm (f=200 mm), R_g=8.5×10⁻⁴ m³/s, n_f=200 f/s

Fig.16　X-ray transmission observation photos of keyhole and/or bubble generation in molten pool during CW YAG laser welding of type 304 steel in Ar, He, and N_2 coaxial shielding gas

Bubbles，resulting in pores or porosity，are normally formed from the tip of a keyhole during laser welding，and thus the following procedures for the reduction in porosity are proposed[9,13,19~21]，and their effectiveness is confirmed：1）full penetration welding；2）proper pulse modulation（Fig. 17)[22,23]；3）forwardly tilted laser beam；4）twin-spots laser welding；5）vacuum welding；6）the use of tornado nozzle；7）hybrid welding with laser and TIG or MIG at high arc current；8）high speed welding，and so on.

A5182 (t=7 mm); CO_2 laser; P_1=5.0 kW, v=25 mm/s, f_d=0 mm, f=100 Hz, coaxial shielding gas: Ar, R_g=5×10⁻⁴ m³/s (nozzle dia.: ϕ8 mm)

duty cycle: D_u=[$a/(a+b)$]×100%

(a) D_u=100% (CW), P_A=5 kW　(b) D_u=90% (CW), P_A=4.5 kW　(c) D_u=80% (CW), P_A=4 kW

(d) D_u=70% (CW), P_A=3.5 kW　(e) D_u=60% (CW), P_A=3 kW　(f) D_u=50% (CW), P_A=2.5 kW
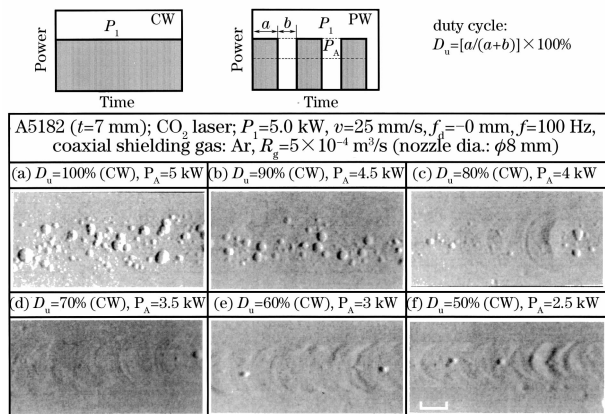
Fig.17　Effect of pulse modulation on porosity in CO_2 laser weld beads of aluminium alloy

In laser welding of Zn-coated steel，it is impor-

tant to control a gap between lapped sheets in order to escape vapors and their pressure due to low evaporation temperature and high vaporization pressure of Zn. Laser brazing can be applied to join Zn-coated steel sheets without porosity or pits[24]. Moreover，laser welding of die cast or sintering alloys is difficult because pores are inevitably formed in weld fusion zones[24].

In some aluminum alloys，cracks occur under some conditions，but do not take place under other conditions. The experimental results concerning the formation conditions of cracking in A7N01 aluminium alloy is shown in Fig.18[25]. It is found that cracking is easily formed at higher welding speeds in thicker plates.

A7N01: P_1=5 kW (CW), f=254 mm, f_d=0 mm, Ar (R_g=5×10⁵ m³/s, ϕ=8 mm)

	25 mm/s	50 mm/s	75 mm/s	100 mm/s	125 mm/s	150 mm/s
1 mmᵗ			○	○	○	○
2 mmᵗ	○	○	○	○	○	○
3 mmᵗ	○	○	○	○	▲	▲
4 mmᵗ	○	○	▲	▲	●	●
5 mmᵗ	○	○	●	●	●	○
6 mmᵗ	○	▲	●	●	●	○

○: no cracking　▲:crack in half sections observed　●:crack in all sections

Fig.18　Effects of plate thickness and welding speed on cracking in A7N01 aluminium alloy welded with a CO_2 laser

In laser welding of aluminum alloys，spattering occurs easily，and consequently an underfilled weld bead can be formed. The surface is modified by applying hybrid welding with MIG arc (as the following heat source)[22,26].

6　Conclusions

Laser welding phenomena are satisfactorily understood. Welding results made with CW lasers are described. In the case of welding with 10.6-μm CO_2 lasers，Ar or N_2 gas plasma are easily formed to absorb laser irradiation energy，while in the case of welding with YAG，disk，or fiber lasers，a tall plume formed exerts an effect of refraction，defocusing，and Rayleigh scattering to reduce penetration. Spattering and humping phenomena are observed due to the effect of laser-induced plume. Porosity is chiefly generated from the tip of a deep keyhole，and some preventive procedures are de-

veloped. Cracking occurs in laser weld metals of thicker plates at high welding speeds.

Acknowledgements　The authors would like to acknowledge Mr. Masami Mizutani, Dr. Naoki Seto, Mr. Keisuke Kinoshita, Mr. Naoyuki Matsumoto, and so on of former Graduate Students, and technical specialist in JWRI of Osaka University.

References

1 S. Katayama. New Developments in Advanced Welding [M]. Ahmed N: 2005, Cambridge England, Woodhead Publishing Limited, p.158～197

2 Y. Kawahito, K. Kinoshita, S. Katayama et al.. Visualization of interaction between laser beam and YAG-laser-induced plume [C]. ICALEO 2005 Congress Proceedings, LIA, 2005, **98**:920～928

3 Y. Kawahito, M. Mizutani, S. Katayama. Elucidation of high-power fiber laser welding phenomena of stainless steel and effect of factors on weld geometry [J]. J. Phys. D: Appl. Phys., 2007, **40**:5854～5859

4 S. Katayama, N. Seto, J. D. Kim et al.. Effect of nitrogen on laser weldability of aluminium alloys [C]. IIW, 1999, IIW Doc No. IX-1949-99

5 N. Seto, S. Katayama, A. Matsunawa. High-speed simultaneous observation of plasma and keyhole behavior during high power CO₂ laser welding: Effect of shielding gas on porosity formation [J]. J. Laser Applications, 2000, **12**(6):245～250

6 Y. Kawahito, K. Kinoshita, N. Matsumoto et al.. Interaction between laser beam and plasma/plume induced in welding of stainless steel with ultra-high power density fiber laser [J]. Q. J. Jpn. Weld. Soc., 2007, **25**(3):461～467

7 S. Katayama, C. D. Lundin. Laser welding of aluminum alloy 5456——laser weldability of aluminum alloys (Report Ⅰ) [J]. J. Light Metal Welding and Construction, 1991, **29**(7):295～307

8 S. Katayama, C. D. Lundin. Laser welding of commercial aluminum alloys——laser weldability of aluminum alloys (Report Ⅱ) [J]. J. Light Metal Welding and Construction, 1991, **29**(8): 349～360

9 A. Matsunawa, K. Kojima, S. Katayama. CO₂ laser weldability of aluminum alloys (Report Ⅰ)——effect of welding conditions on melting characteristics [J]. J. Light Metal Welding and Construction, 1997, **35**(10):461～472

10 S. Katayama, Y. Kawahito, K. Kinoshita et al.. Weld penetration and phenomena in 10 kW fiber laser welding [C]. ICALEO 2007 Congress Proceedings (Proc. 26th International Congress on Applications of Lasers &. Electro-Optics), Orlando, LIA, 2007, **100**:353～359

11 K. Kinoshita, M. Mizutani, Y. Kawahito et al.. Phenomena of welding with high-power fiber laser [C]. ICALEO 2006 Congress Proceedings (25th International Congress on Applications of Lasers &. Electro-Optics), Scottsdale, LIA, 2006, **99** Paper # 902:535～542

12 A. Matsunawa, N. Seto, J. D. Kim et al.. Observation of keyhole and molten pool behaviour in high power laser welding——

mechanism of porosity formation and its suppression method [J]. Trans. of JWRI, 2001, **30**(1):13～27

13 N. Seto, S. Katayama, A. Matsunawa. High-speed simultaneous observation of plasma and keyhole behavior during high power CO₂ laser welding: effect of shielding gas on porosity formation [J]. J. Laser Applications, 2000, **12**(6):245～250

14 A. Matsunawa, J. D. Kim, S. Katayama et al.. Spectroscopic studies on laser-induced plume of aluminum alloys [C]. Proc. ICALEO '95, San Diego, LIA, 1995, **80**:719～728

15 S. Katayama, Y. Kawahito, M. Mizutani. Collaboration of physical and Metallurgical viewpoints for understanding and process development of laser welding [C]. ICALEO 2007 Congress Proceedings (Proc. 26th International Congress on Applications of Lasers &. Electro-Optics), Orlando, LIA, 2007, **100** ♯701: 360～369

16 Y. Kawahito, K. Kinoshita, N. Matsumoto et al.. High-speed observation and spectroscopic analysis of laser-induced plume in high-power fiber laser welding of stainless steel [J]. Q. J. Jpn. Weld. Soc., 2007, **25**(3):455～460

17 S. Katayama, S. Oiwa, H. Ishida et al.. Effect of laser-induced plume on laser beam focusing during remote welding [C]. 61st Annual Assembly of Int. Inst. Welding (IIW), Graz, IIW Doc. IV-962-08

18 S. Katayama, Y. Kawahito, M. Mizutani. Effect of gas compositions on laser weldability of stainless steel [C]. Proc. the 69th Laser Materials Processing Conference, 2007, **69**:161～170

19 S. Katayama, Y. Kobayashi, N. Seto et al.. Effect of vacuum on penetration and defects in laser welding [C. Proc. Laser Materials Processing Conference ICALEO 2000, LIA, USA, 2000, **89**:Section C 182～191

20 S. Katayama, N. Seto, J. D. Kim et al.. Formation mechanism and reduction method of porosity in laser welding of stainless steel [C]. Proc. ICALEO '97, San Diego, USA, 1997, **83**:Part 2 Section G 83～92

21 S. Katayama, N. Seto, J. D. Kim et al.. Formation mechanism and suppression procedure of porosity in high power laser welding of aluminum alloys [C]. Proc. ICALEO '98, LIA, Orlando, USA, 1998, **85**:Section C 24～33

22 S. Uchiumi, J. B. Wang, S. Katayama et al.. Penetration and welding phenomena in YAG laser-MIG hybrid welding of aluminum alloy [C]. ICALEO 2004 Congress Proceedings, San Francisco, LIA, 2004, **97**:530

23 S. Katayama, A. Matsunawa. Laser weldability of aluminum alloys [C]. Proc. the 69th Laser Materials Processing Conference, 1998, **43**:33～52

24 S. Katayama, Y. Kawahito, M. Mizutani. Welding phenomena and results in laser joining of various materials [C]. Proc. the 66th Laser Materials Processing Conference, 2006, **66**:1～8

25 S. Katayama, A. Matsunawa. Laser weldability of aluminum alloys [C]. Proc. the 69th Laser Materials Processing Conference, 1998, **43**:33～52

26 H. Nagayama, M. Mizutani, Y. Kawahito et al.. Weld penetration and welding phenomena of aluminum alloy with high-power fiber laser [C]. ICALEO 2007 Congress Proceedings (Proc. 26th International Congress on Applications of Lasers &. Electro-Optics), Orlando, LIA, 2007, **100**:916～924